Reductive Half-Reaction of Medium-Chain Fatty Acyl-CoA Dehydrogenase Utilizing Octanoyl-CoA/Octenoyl-CoA as a Physiological Substrate/Product Pair: Similarity in the Microscopic Pathways of Octanoyl-CoA Oxidation and Octenoyl-CoA Binding†

N. Ravi Kumar and D. K. Srivastava*

Biochemistry Department, North Dakota State University, Fargo, North Dakota 58105

Received April 6, 1994; Revised Manuscript Received May 19, 1994®

ABSTRACT: Of the different chain length fatty acyl-CoA substrates, octanoyl-CoA has been known as one of the most efficient (and physiological) substrates for the medium-chain fatty acyl-CoA dehydrogenase (MCAD)-catalyzed reaction. The reaction of MCAD–FAD with octanoyl-CoA ([MCAD–FAD] ≪ [octanoyl-CoA]), measured via the stopped-flow technique, at 5 °C was characterized by a biphasic decrease and increase in absorptions at 450 and 545 nm, respectively. The average values of the fast ($1/\tau_1$) and slow ($1/\tau_2$) relaxation rate constants, derived from the data at these wavelengths, were found to be 319.7 ± 33.5 and 28.8 ± 12.5 s^{-1}, respectively, and both of these relaxation rate constants remained invariant between 8 and 200 μM concentrations of octanoyl-CoA. Under identical experimental conditions, we measured time courses for the interaction of MCAD–FAD with octenoyl-CoA ([MCAD–FAD] ≪ [octenoyl-CoA]) by monitoring the absorption changes at 299, 394, and 440 nm. The binding profile was consistent with a biphasic decrease (at 440 nm) and increase (at 299 and 394 nm) in absorbance, with similar magnitudes of fast [$1/\tau_1$ (average) = 382.3 ± 39.8 s^{-1}] and slow [$1/\tau_2$ (average) = 14.3 ± 7.4 s^{-1}] relaxation rate constants. The observed relaxation rate constants were, once again, found to be invariant with changes in the octenoyl-CoA concentration from 40 to 150 μM. In addition, the dissociation rate constant of octenoyl-CoA from the MCAD–FAD–octenoyl-CoA complex (10.3 ± 0.2 s^{-1}) was found to be similar to the overall rate constant (7.1 ± 0.1 s^{-1}) for the release of octanoyl-CoA from the MCAD–$FADH_2$–octenoyl-CoA complex (via reversal of the redox reaction). These results attest to a marked similarity in the microscopic pathways of the enzyme-catalyzed oxidation of octanoyl-CoA (i.e., the chemical transformation reaction) and the enzyme–octenoyl-CoA interaction (leading to changes in the electronic structure of FAD). The reductive half-reaction of the enzyme involving octanoyl-CoA vis-à-vis other acyl-CoA substrates led to the following conclusions: (1) Unlike other substrates, the octanoyl-CoA-dependent redox reaction does *not* limit the overall rate of MCAD catalysis. (2) The higher yield of the reduced enzyme species (80–85%) in the presence of octanoyl-CoA substrate is due to an additional protein isomerization during the reductive half-reaction; this step is absent with other substrates. (3) Due to a slow exchange of octenoyl-CoA by octanoyl-CoA from the MCAD–$FADH_2$–octenoyl-CoA complex, the oxidase activity of the enzyme is drastically suppressed. The role of protein conformational changes during the course of ligand binding and/or catalysis is discussed.

Medium-chain fatty acyl-CoA dehydrogenase (MCAD[1]) catalyzes the conversion of different chain length fatty acyl-CoA's into their corresponding *trans*-enoyl-CoA moieties via two consecutive sequences of steps [for reviews, see Beinert (1963a) and Engel (1990)]. The first step involves the concerted abstraction of a proton and a hydride ion from the α- and β-carbon chains of the fatty acyl-CoA substrates, concomitant with the reduction of the enzyme (E)-bound FAD to $FADH_2$. The reoxidation of E–$FADH_2$, to propagate further rounds of catalysis, is accomplished via transfer of electrons to a variety of organic electron acceptors (Engel, 1990); the natural electron acceptor for this process, under physiological conditions, is the electron-transferring flavoprotein (ETF; Beinert, 1963b) (eq 1). The enzyme is known to

$$\text{E–FAD} + \text{acyl-CoA} \rightleftharpoons \text{E–}FADH_2\text{–enoyl-CoA} \quad (1A)$$

$$\text{E–}FADH_2\text{–enoyl-CoA} + \text{ETF–FAD} \rightleftharpoons \text{E–FAD–enoyl-CoA} + \text{ETF–}FADH_2 \quad (1B)$$

exhibit a fairly broad range of substrate specificity, catalyzing the oxidation of aliphatic-CoA substrates ranging from chain length C_4 (butyryl-CoA) to C_{16} (palmitoyl-CoA) (Beinert & Page, 1957; Hall et al., 1979). Of these, C_8 (octanoyl-CoA) through C_{10} (decanoyl-CoA) are oxidized by the enzyme with maximum efficiencies, and thus they are considered to be the physiological substrates for the MCAD-catalyzed reaction (Crane et al., 1956; Hall, et al., 1979). The ratio of k_{cat} to K_m (octanoyl-CoA) has been measured to be 1.64×10^7 M^{-1} s^{-1} when utilizing ETF as the electron acceptor (Beinert, 1963a).

Besides aliphatic acyl-CoA substrates, MCAD catalyzes the oxidation of a variety of aromatic/heterocyclic ring-

† Journal article no. 2177 of the North Dakota Agricultural Experiment Station. Work was supported by the American Heart Association, Dakota Affiliate.

* Author to whom correspondence should be addressed.

® Abstract published in *Advance ACS Abstracts,* July 1, 1994.

[1] Abbreviations: MCAD, medium-chain fatty acyl-coenzyme A dehydrogenase; IPCoA, 3-indolepropionyl-coenzyme A; IACoA, *trans*-3-indoleacryloyl-coenzyme A; $FcPF_6$, ferricenium hexafluorophosphate; FAD, flavin adenine dinucleotide; $FADH_2$, reduced flavin adenine dinucleotide; ETF, electron-transferring flavoprotein; OcaCoA, octanoyl-coenzyme A; OceCoA, octenoyl-coenzyme A; AcAcCoA, acetoacetyl-coenzyme A.

0006-2960/94/0433-8833$04.50/0

substituted propionyl-CoA substrates, such as indolepropionyl-CoA (Johnson et al., 1992), furylpropionyl-CoA (McFarland et al., 1982), hydrocinnamoyl-CoA (Murfin, 1974), etc. The major advantage of utilizing these substrates is that their corresponding reaction products (α,β unsaturated enoyl-CoA's) are the colored species, and thus they are readily detectable by UV/visible absorption spectroscopy (Johnson et al., 1992; Johnson & Srivastava, 1993). This feature prompted us, as well as others, to monitor the enzyme-catalyzed reaction progress without recourse to the spectral signals of flavin or other colored electron acceptors (Johnson et al., 1992, 1994; McFarland et al., 1982; Yao & Schultz, 1993).

We introduced indolepropionyl/indoleacryloyl-CoA as a competent substrate/product pair for MCAD (Johnson et al., 1992). The catalytic efficiency of the enzyme (as judged by the ratio of k_{cat}/K_m) utilizing IPCoA as substrate (4×10^4 M^{-1} s^{-1}) has been found to be comparable to that of butyryl-CoA (5.3×10^4 M^{-1} s^{-1}; Johnson et al., 1992), the most frequently utilized substrate for the mechanistic investigation of this enzyme (McKean et al., 1979; Schopfer et al., 1988). While utilizing IPCoA as substrate, we discerned that the MCAD catalyzes both dehydrogenation (in the presence of organic electron acceptors) as well as oxidation (O_2 being the terminal electron acceptor) reactions (Johnson et al., 1992, 1994). These reactions were found to differ not only with respect to the nature of the electron acceptor but also with respect to the overall microscopic pathways (Johnson & Srivastava, 1993). Like the dehydrogenation reaction, the oxidation reaction exhibited Michaelian dependence on the IPCoA concentrations, albeit the K_m (for IPCoA) and k_{cat} values for the latter reaction were found to be about 1 order of magnitude lower than those for the former reaction (Johnson et al., 1992). A relationship between the macroscopic and microscopic parameters for the oxidation reaction has recently been established (Johnson et al., 1994).

By utilizing the chromophoric potential of IACoA, we investigated the influence of the resident environment of the enzyme site phase on the electronic spectrum of IACoA (Johnson et al., 1992). Such studies revealed that the electronic spectrum of IACoA is red shifted upon interaction with both the reduced and oxidized forms of the enzyme. In contrast, the spectrum of the enzyme-bound FAD is blue shifted with a marked hyperchromicity. These spectral changes were ascribed to originate due to the polarization of the carbonyl group of IACoA within the enzyme site phase, and the lowering of the enzyme site polarity around the flavin region (Johnson et al., 1992). Transient kinetic investigation of the interaction of E–FAD and IACoA revealed that the overall process proceeds in two steps. The first (fast) step involves the formation of an E–FAD–IACoA collision complex, which is slowly isomerized in the second step (Johnson et al., 1992). Of these, the latter step accompanied changes in the electronic spectra of both the FAD and IACoA species within the E–FAD–IACoA complex; no spectral changes (of either of these chromophoric species) occurred within the collision complex (eq 2A; Johnson et al., 1992). An identical scenario emerged while we were investigating the reductive half-reaction of the enzyme, utilizing IPCoA as the enzyme substrate. The reaction proceeded via the formation of a Michaelian complex, which is slowly isomerized to an intermediary complex, denoted X (eq 2B). The latter complex was characterized by the electronic spectra of IACoA (albeit red shifted to 33 nm with respect to aqueous IACoA) and the reduced flavin moiety (Johnson & Srivastava, 1993).

$$\text{E–FAD} + \text{IACoA} \rightleftharpoons \text{E–FAD–IACoA} \rightleftharpoons \text{E–FAD*–IACoA**} \quad (2A)$$

$$\text{E–FAD} + \text{IPCoA} \rightleftharpoons \text{E–FAD–IPCoA} \rightleftharpoons \text{X(E–FADH}_2\text{–IACoA)*} \quad (2B)$$

In this way, the slow isomerization step, once again, accompanied the formation of a highly conjugated IACoA species (eq 2B). The only difference between these two seemingly different processes is that the slow step of eq 2A is devoid of "chemistry", whereas that of eq 2B is coupled to the oxidation/reduction reaction (Johnson et al., 1994). Hence, it appears likely that the microscopic pathway of the enzyme-catalyzed chemical transformation is similar to that of the enzyme–enoyl-CoA interaction.

A question arose immediately concerning whether the above feature is an intrinsic property of the IPCoA/IACoA as the pseudo substrate/product pair of the enzyme or is a property of all of the other acyl-CoA/enoyl-CoA pairs in general. While pondering this possibility, we realized that despite the recognition that octanoyl-CoA is one of the most efficient (and physiological) substrates for the enzyme, very little attempt has been made toward elucidation of its detailed oxidoreductive pathway (Hall et al., 1979). Besides, octanoyl-CoA has been well recognized to be a substrate that yields an unusually stable MCAD–$FADH_2$–octenoyl-CoA complex, which is resistant to oxidation by molecular oxygen (Beinert & Page, 1957). With these limitations in mind, we undertook a detailed kinetic investigation of the MCAD-catalyzed oxidation of octanoyl-CoA and the enzyme-octenoyl interaction under identical experimental conditions. As will be elaborated subsequently, such investigations have thrown significant light on the structural–functional aspects of this enzyme.

MATERIALS AND METHODS

Materials

Coenzyme A, glucose oxidase (type VIII), EDTA, octanoyl-CoA, and acetoacetyl-CoA were purchased from Sigma. All other reagents were of analytical reagent grade.

Methods

All experiments were performed in a standard 50 mM potassium phosphate buffer (pH 7.6) containing 0.3 mM EDTA at 25 °C, unless stated otherwise.

Pig kidney MCAD was purified in our laboratory and assayed as described by Johnson et al. (1992). The active enzyme concentration was determined in terms of flavin content by using an extinction coefficient of 15.4 mM^{-1} cm^{-1} at 446 nm (Thorpe et al., 1979).

Preparation of Octenoyl-CoA. Octenoyl-CoA was prepared enzymatically, in the above buffer system, by following the MCAD-catalyzed conversion of octanoyl-CoA in the presence of $FcPF_6$. A typical reaction mixture (total volume = 5 mL) containing 1 mM octanoyl-CoA and 2 mM $FcPF_6$ was incubated with 1 μM MCAD for 30 min at room temperature. The solution was centrifuged to remove the (insoluble) reduced form of the electron acceptor. To the clear supernatant were added additional amounts of $FcPF_6$ (0.7 mM) and MCAD (0.5 μM), and the mixture was incubated for an additional 20 min. The solution was subsequently filtered through a 0.45-μm membrane filter and then loaded onto a C_{18} HPLC preparatory column (Alltech, 25 cm × 1 cm i.d.) that was preequilibrated with a 20 mM phosphate buffer (pH 7.0).

The column was first washed with the above buffer for 5 min. After this, a gradient of 20 mM potassium phosphate (100% in A) to pure methanol (100% in B) was applied over 45 min, and the elution profile was monitored at 254 nm. Octenoyl-CoA eluted as a major peak from this column, which corresponded to the elution profile of octenoyl-CoA prepared by the mixed anhydride method (Bernert & Sprecher, 1977). The elution peak of the un-reacted octanoyl-CoA just followed that of octenoyl-CoA. To avoid contamination by octanoyl-CoA in our octenoyl-CoA preparation, we checked the individual fractions by rechromatography on an analogous C_{18} HPLC analytical column (Alltech, 25 cm × 0.46 cm i.d.). Only fractions that were devoid of any shoulder peak due to octanoyl-CoA contamination were pooled. From these pooled fractions, methanol was removed on a rotatory evaporator, and the resultant aqueous solution (containing octenoyl-CoA) was stored at −20 °C. The gradient applied on the analytical column was 20 mM potassium phosphate (pH 7.0) (75% in A) to pure methanol (80% in B) over 20 min.

The extinction coefficient of octenoyl-CoA was determined by measuring the amounts of thiol released upon hydrolysis by 1 M hydroxylamine (pH 7.0) for 30 min at 37 °C. The thiol groups released were estimated by the DTNB method (Ellman, 1959). The amount of thiol released was correlated with the absorption of octenoyl-CoA at 258 nm. The extinction coefficient of *trans*-octenoyl-CoA thus determined was 20.4 mM^{-1} cm^{-1} at 258 nm. The extinction coefficient of octanoyl-CoA at 259 nm was taken to be 15.6 mM^{-1} cm^{-1} (Johnson et al., 1992).

Spectral data acquisitions were performed on Perkin-Elmer Lambda 3B and Beckmann 7400 diode array spectrophotometers.

Transient Kinetic Experiments. The transient kinetic experiments were performed on an Applied Photophysics MV-14 sequential mixing stopped-flow system (optical path length = 10 mm, dead time = 1.34 ms). This device was used in single as well as in double (sequential) mixing modes. In the single mixing mode, the contents of both syringes were diluted by 50%, whereas in the double mixing mode, the contents of syringes 1 and 2 were diluted by 75% and the content of syringe 3 was diluted by only 50%.

Anaerobic Experiments. Buffers and solutions were made anaerobic by bubbling and degassing in 4 × 15-min cycles with oxygen-free argon, as described by Johnson et al. (1993). Immediately prior to using these reagents in the stopped-flow system, glucose oxidase and glucose were added to concentrations of 30 μg/mL and 0.8 mM, respectively, to remove any traces of oxygen. The stopped-flow instrument was made anaerobic by flushing the cuvette, lines, and syringes with 5 mM sodium dithionite solution for 3 h, followed by thorough flushing of the entire system with anaerobic buffer.

RESULTS

Reaction of MCAD–FAD and Octanoyl-CoA. Beinert and his collaborators first recognized that the reaction of MCAD–FAD with octanoyl-CoA results in the formation of an unusually stable (toward oxidation by O_2) MCAD–$FADH_2$–octenoyl-CoA complex (Beinert & Page, 1957), which is characterized by a lower absorption at 450 nm and a broad charge transfer band around 500–700 nm (Beinert, 1963a). The stability of the MCAD–$FADH_2$–octenoyl-CoA complex restricts the reaction of MCAD–FAD and octanoyl-CoA to essentially a single turnover condition, even under aerobic buffer conditions. Taking advantage of these features, we measured the time-dependent absorption changes at 450 nm upon mixing 1.5 μM MCAD–FAD with 83 μM octanoyl-CoA and at 545 nm upon mixing 10 μM MCAD–FAD with 150 μM octanoyl-CoA (in 50 mM phosphate buffer, pH 7.6, at 5 °C) via the stopped-flow syringes. As shown in Figure 1, the reaction progress is characterized by a decrease in absorption at 450 nm and an increase in absorption at 545 nm. These kinetic traces are best fit by a two-exponential rate equation, with fast ($1/\tau_1$) and slow ($1/\tau_2$) relaxation rate constants equal to 315.6 ± 32.0 and 33.7 ± 11.4 s^{-1} at 450 nm (decreasing phase) and 329.9 ± 48.5 and 16.5 ± 0.2 s^{-1} at 545 nm (increasing phase), respectively. Note that although the fast relaxation rate constants at these wavelengths are more or less the same, the slow relaxation rate constant at 450 nm is about 2-fold higher than that observed at 545 nm. We have repeatedly observed such a discrepancy in different sets of experiments, and we believe that its origin lies in a slight increase in absorption at the 450-nm region (due to formation of the charge transfer complex) during the second relaxation phase. The average values of both the fast and slow relaxation rate constants at 450 and 545 nm were calculated to be 319.7 ± 33.5 and 28.8 ± 12.5 s^{-1}, respectively. Besides these two phases, no other relaxation phase was observed within the 100-s time regime. However, if the reaction was allowed to proceed for several hours, two additional relaxation phases, characterized by the slow disappearance of the charge transfer band, were discerned (data not shown). As will be elaborated

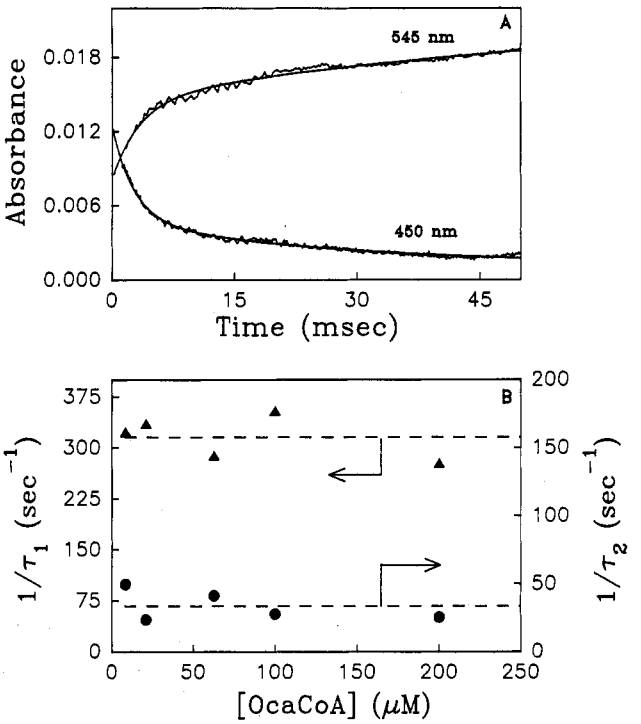

FIGURE 1: Reductive half-reaction of MCAD in the presence of octanoyl-CoA. Panel A shows the representative stopped-flow traces for the reaction of MCAD–FAD with octanoyl-CoA (50 mM phosphate buffer, pH 7.6, at 5 °C) in the flavin (450 nm) and charge transfer (545 nm) regions. The after mixing concentrations of MCAD–FAD and octanoyl-CoA were 0.75 and 41.5 μM, respectively, for the reaction at 450 nm and 5 and 75 μM, respectively, for the reaction at 545 nm. The solid smooth lines are the best fits of the experimental data according to the two-exponential rate equations for decreasing (450 nm) and increasing (545 nm) phases. The fast ($1/\tau_1$) and slow ($1/\tau_2$) relaxation rate constants obtained from the best fit of the experimental data were 376.5 ± 14.9 and 38.1 ± 4.0 s^{-1}, respectively, at 450 nm and 295.6 ± 16.2 and 16.6 ■ 0.9 s^{-1}, respectively, at 545 nm. Panel B shows the octanoyl-CoA-dependent (after mixing concentrations) fast ($1/\tau_1$, ▲) and slow ($1/\tau_2$, ●) relaxation rate constants for the reaction measured at 450 nm.

in a separate communication, these latter phases are responsible for the slow oxidase activity of the enzyme.

A casual comparison of the kinetic pattern of Figure 1 vis-à-vis those obtained with either indolepropionyl-CoA or butyryl-CoA as substrate (Johnson & Srivastava, 1993; Schopfer et al., 1988) reveals that the biphasic increase in absorption at the 545-nm region is unique for the octanoyl-CoA substrate. The reductive half-reactions of the enzyme utilizing either indolepropionyl-CoA or butyryl-CoA as substrates are characterized by a single-exponential increase followed by a decrease in absorption in the charge transfer region (Johnson & Srivastava, 1993; Schopfer et al., 1988). The amplitudes of the absorption changes at 450 nm (due to the reduction of MCAD–FAD by octanoyl-CoA) during the fast and slow phases (Figure 1) are about 60% and 40%, respectively. The total reduction of the enzyme-bound flavin by octanoyl-CoA was found to be between 80% and 85%. This is in contrast to about a 56% reduction of flavin when butyryl-CoA is utilized as the enzyme substrate (Crane et al., 1956). Thus, it appears evident that the thermodynamic drive of the second (slow) phase (in the case of octanoyl-CoA) results in a higher yield (80–85%) of the reduced enzyme species involving octanoyl-CoA as the substrate, but not with butyryl-CoA and IPCoA substrates (see Discussion).

We measured the magnitudes of the fast ($1/\tau_1$) and slow ($1/\tau_2$) relaxation rate constants as a function of octanoyl-CoA concentration ([MCAD–FAD] $\ll$ [octanoyl-CoA]) under the experimental conditions of Figure 1A. As shown in Figure 1B, both $1/\tau_1$ and $1/\tau_2$ remain unaffected upon variation of the octanoyl-CoA concentration from 8 to 200 μM. This (zero-order) dependence is a reflection of the fact that the enzyme remains saturated within the above concentration ranges of octanoyl-CoA. An upper limit of the dissociation constant for the MCAD–FAD–octanoyl-CoA complex can be set at 0.8 μM. We could not perform experiments at lower concentrations of octanoyl-CoA (while maintaining pseudo-first-order conditions) due to limitations in the absorption signal. Although this experimental constraint precluded us from formulating a quantitative model of the overall reaction, some qualitative predictions have been made (see Discussion).

Binding of Octenoyl-CoA with MCAD–FAD. We examined the interaction of MCAD–FAD with the reaction product, octenoyl-CoA. The latter was prepared by the MCAD-catalyzed conversion of octanoyl-CoA in the presence of ferricenium hexafluorophosphate and purified to homogeneity on a preparatory C_{18} HPLC column (see Materials and Methods). The enzymatic method for the preparation of octenoyl-CoA was preferred over the chemical method (i.e., thioesterification of 2-octenoic acid; Bernert & Sprecher, 1977), since the latter preparation was found to be contaminated by some species that coeluted (as a shoulder band) with octenoyl-CoA from the HPLC column, and the resultant preparation was found to slowly bleach the 450-nm band of MCAD–FAD. No such shoulder band was detected in the enzymatically prepared octenoyl-CoA, and the flavin bleaching property of the product was reduced by about 1 order of magnitude (data not shown); the half-life of the latter process was found to be 4 h.

Figure 2A shows the spectra of MCAD–FAD and MCAD–FAD–octenoyl-CoA (prepared by the immediate addition of octenoyl-CoA to the MCAD–FAD solution); the total time of mixing (accomplished with the aid of a magnetic stirrer installed under the cuvette) and the spectral acquisition (by a diode array spectrophotometer) was less than 5 s. Note

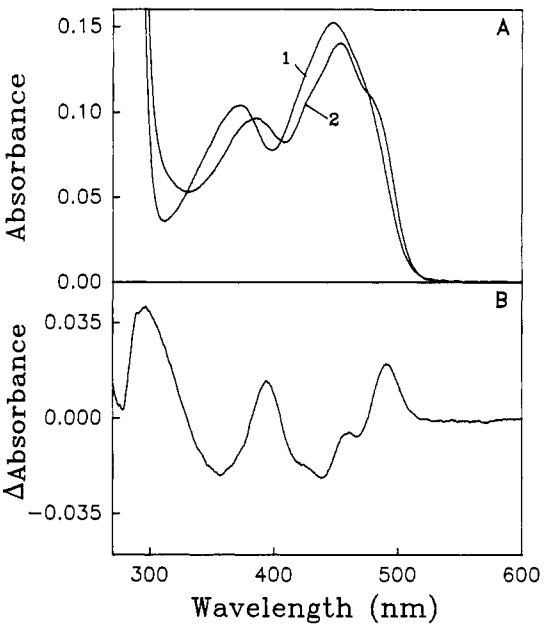

FIGURE 2: Octenoyl-CoA-induced spectrum of MCAD–FAD. Panel A shows the spectra of MCAD–FAD (10 μM) in the absence (curve 1) and presence (curve 2) of 20 μM octenoyl-CoA, in 50 mM phosphate buffer (pH 7.6) at 25 °C. Panel B shows the difference spectrum, i.e., the spectrum of the mixture minus the spectra of the individual species.

that the spectra of MCAD–FAD and MCAD–FAD–octenoyl-CoA are characterized by four isosbestic points at 330, 382, 406, and 476 nm, respectively. The flavin band of MCAD–FAD within the complex is red shifted with the concomitant appearance of a shoulder band around 491 nm. The overall spectral changes are evident from the difference spectrum, i.e., the spectrum of MCAD–FAD–octenoyl-CoA minus the spectra of MCAD–FAD and octenoyl-CoA (Figure 2B). Note that the difference spectrum is marked by three positive bands at 299, 394, and 491 nm and two negative bands at 356 and 440 nm, respectively. Of these, the absorption band at 299 nm is the most pronounced and thus was used for the octenoyl-CoA concentration-dependent transient kinetic investigations (see following sections).

Figure 3A shows the time-dependent increases in absorption at 299 and 394 nm and the decrease in absorption at 440 nm upon mixing MCAD–FAD with at least 7.5-fold higher concentrations of octenoyl-CoA (in 50 mM phosphate buffer, pH 7.6, at 5 °C) via the stopped-flow syringes. These kinetic traces were best fit (solid lines) by the two-exponential rate equations for the increases in absorption at 299 and 394 nm and the decrease in absorption at 440 nm. The fast ($1/\tau_1$) and slow ($1/\tau_2$) relaxation rate constants obtained from the best fit of the experimental data were found to be 477.8 ± 13.0 and 13.9 ± 1.0 s^{-1} at 299 nm; 353.6 ± 5.7 and 11.7 ± 0.1 s^{-1} at 394 nm; and 378.0 ± 8.0 and 35.2 ± 5.0 s^{-1} at 440 nm, respectively. The average values of the fast and slow relaxation rate constants were found to be 382.3 ± 39.8 and 14.3 ± 7.4 s^{-1}, respectively. It should be pointed out that the magnitudes of these relaxation rate constants are similar to the corresponding fast and slow relaxation rate constants obtained during the reaction of MCAD–FAD with octanoyl-CoA (see Figure 1). However, unlike the latter case, the amplitudes of the absorption changes during the fast and slow phases of the MCAD–FAD + octenoyl-CoA interaction were found to be 75% and 25%, respectively.

We measured the octenoyl-CoA concentration-dependent magnitudes of the fast and slow relaxation rate constants (while

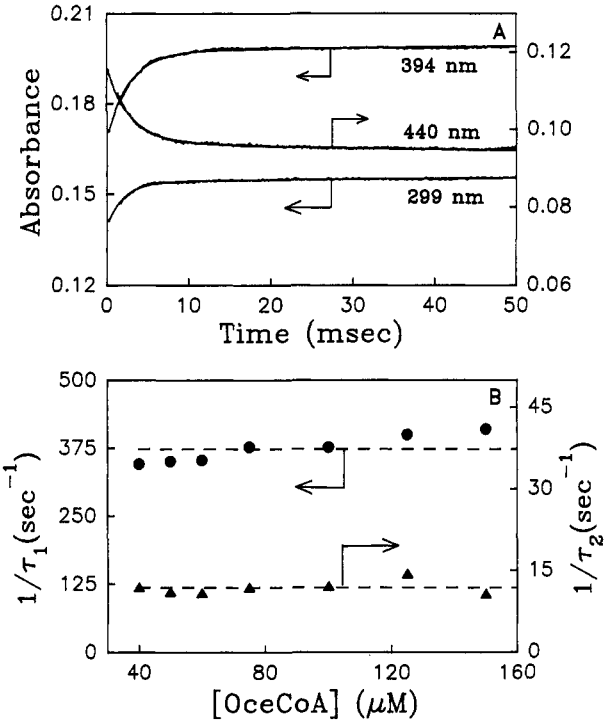

FIGURE 3: Transient kinetics for the interaction of MCAD–FAD with octenoyl-CoA. Panel A shows the time-dependent changes in absorption upon mixing MCAD–FAD with octenoyl-CoA via the stopped-flow syringes, under precisely the experimental conditions of Figure 1. Solid smooth lines are the best fits of the experimental data according to the two-exponential rate equations for decreasing (440 nm) and increasing (299 and 394 nm) phases. The (after mixing) concentrations of MCAD–FAD and octenoyl-CoA and the associated rate constants for the individual traces are as follows: 394-nm trace, [MCAD–FAD] = 20 μM, [octenoyl-CoA] = 150 μM, $1/\tau_1$ = 353.6 ± 5.7 s^{-1}, $1/\tau_2$ = 11.7 ± 0.1 s^{-1}; 299-nm trace, [MCAD–FAD] = 5 μM, [octenoyl-CoA] = 150 μM, $1/\tau_1$ = 477.8 ± 13.0 s^{-1}, $1/\tau_2$ = 13.9 ± 1.0 s^{-1}; 440-nm trace, [MCAD–FAD] = 10 μM, [octenoyl-CoA] = 75 μM, $1/\tau_1$ = 378.0 ± 8.0 s^{-1}, $1/\tau_2$ = 35.2 ± 5.0 s^{-1}. Panel B shows the octenoyl-CoA (after mixing) concentration-dependent fast ($1/\tau_1$, ●) and slow ($1/\tau_2$, ▲) relaxation rate constants measured from the reaction traces at 299 nm.

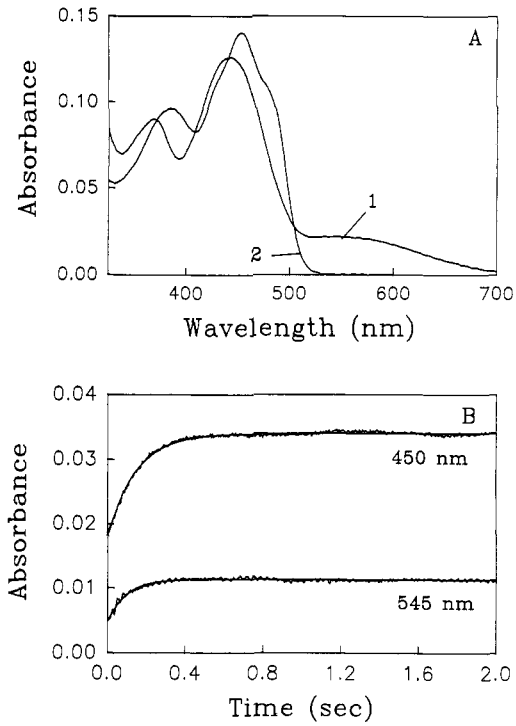

FIGURE 4: Panel A: Comparative spectral features of the MCAD–FAD–acetoacetyl-CoA (curve 1) and MCAD–FAD–octenoyl-CoA (curve 2) complexes. For curve 1: [MCAD–FAD] = 10 μM, [acetoacetyl-CoA] = 88 μM. For curve 2: [MCAD–FAD] = 10 μM, [octenoyl-CoA] = 20 μM. Panel B: Representative stopped-flow traces for the dissociation of octenoyl-CoA/octanoyl-CoA by acetoacetyl-CoA from the MCAD–FAD–octenoyl-CoA (trace at 545 nm) and MCAD–FADH$_2$–octenoyl-CoA (trace at 450 nm) complexes. The dissociation of octenoyl-CoA from the MCAD–FADH$_2$–octenoyl-CoA complex was performed via the single mixing stopped-flow mode. A reaction mixture containing 10 μM MCAD–FAD + 11 μM octanoyl-CoA (syringe 1) was mixed with 1 mM acetoacetyl-CoA (syringe 2), and the time-dependent absorption changes were recorded at 450 nm. The after mixing concentrations of MCAD–FAD, octenoyl-CoA, and acetoacetyl-CoA were 5, 5.5, and 500 μM, respectively. The solid smooth line is the best fit of the experimental data for a single-exponential rate law, with a rate constant of 7.1 ● 0.1 s^{-1}. The dissociation of octenoyl-CoA from the MCAD–FAD–octenoyl-CoA complex by acetoacetyl-CoA was performed via the double mixing stopped-flow mode, and time-dependent reaction progress was recorded at 545 nm. A solution of 25 μM MCAD–FAD (syringe 1) was first mixed with 50 μM octenoyl-CoA (syringe 2) and allowed to age for 2 s in the aging loop. After this time period, 1200 μM acetoacetyl-CoA was mixed via syringe 3, and the time-dependent increase in absorption was recorded at 545 nm. The after mixing concentrations of MCAD–FAD, octenoyl-CoA, and acetoacetyl-CoA were 6.25, 12.5, and 600 μM, respectively. The solid smooth line is the best fit of the experimental data for the single-exponential increase in absorbance, with a rate constant of 10.3 ± 0.2 s^{-1}.

maintaining [MCAD–FAD] ≪ [octenoyl-CoA]) under the experimental conditions of Figure 1. As shown in Figure 3B, these relaxation rate constants remained unaffected upon variation of the octenoyl-CoA concentration from 40 to 150 μM. It is noteworthy that this dependence is similar to that observed from the data of Figure 1B.

Dissociation of Octenoyl-CoA from the Oxidized (MCAD–FAD) and Reduced (MCAD–FADH$_2$) Enzyme Sites. We realized that a neutral CoA derivative such as acetoacetyl-CoA (which serves as neither substrate nor product) can be utilized to displace enoyl-CoA's from the enzyme site, and the rate of such displacement can be taken to be a measure of the overall off rate constant of the enzyme–enoyl-CoA complex (Johnson et al., 1992). Figure 4 (panel A) shows the comparative spectral features of the MCAD–FAD–acetoacetyl-CoA and MCAD–FAD–octenoyl-CoA complexes. Note that the former complex is characterized by a pronounced charge transfer band at 545 nm, which is absent from the MCAD–FAD–octenoyl-CoA complex. Hence, upon mixing MCAD–FAD–octenoyl-CoA with an excessive concentration of acetoacetyl-CoA, the absorption at 545 nm would increase, and the time course of such an increase would provide a measure of the off rate constant for the dissociation of octenoyl-CoA from the MCAD–FAD–octenoyl-CoA complex. However, we realized that such a measurement required a double mixing approach, since the incubation of MCAD–FAD with octenoyl-CoA slowly produced the species that had the property of the bleached flavin band (data not shown). In this double mixing mode, 25 μM MCAD–FAD was first mixed with 50 μM octenoyl-CoA via the two stopped-flow syringes and allowed to age for 2 s (for attainment of the enzyme–octenoyl-CoA equilibrium), followed by mixing with 1200 μM acetoacetyl-CoA via the third stopped-flow syringe. Figure 4 (panel B) shows the time-dependent increase in absorption at 545 nm due to displacement of the enzyme-bound octenoyl-CoA by acetoacetyl-CoA. The reaction profile was best fit by a single-exponential rate equation, with a rate constant of 10.3 ± 0.2 s^{-1}. The observed rate constant was found to be unaffected between 200 and 600 μM acetoacetyl-CoA (after mixing) concentrations.

We observed that when the reaction mixture containing MCAD–FAD and octanoyl-CoA was mixed with acetoacetyl-

CoA, the absorption at 450 nm increases without any significant change in the absorption in the charge transfer complex region (data not shown). As will be elaborated in a subsequent communication, this feature is a result of the reversal of the redox equilibrium toward the MCAD–FAD–octanoyl-CoA complex, followed by the displacement of octanoyl-CoA by acetoacetyl-CoA (see eq 6A). For this composite process, we measured the time-dependent changes in absorption at 450 nm upon mixing 10 μM MCAD–FAD plus 11 μM octanoyl-CoA (syringe 1) with 1000 μM acetoacetyl-CoA (syringe 2) via the stopped-flow syringes. The reaction progress was found to be consistent with a single-exponential increase in absorption (Figure 4, panel B), with a rate constant equal to 7.1 ± 0.1 s^{-1}. This rate constant was found to remain unaffected upon variation in the (after mixing) acetoacetyl-CoA concentration between 200 and 500 μM (data not shown). This attested to the fact that the observed rate constant is a measure of the aggregated rate constant for the conversion of octenoyl-CoA to octanoyl-CoA, followed by its dissociation (see eq 6A). It should be pointed out that this rate constant is, once again, similar to that observed for the dissociation of octenoyl-CoA from the stable form of the MCAD–FAD–octenoyl-CoA complex (see eq 6B).

DISCUSSION

The experimental results presented herein are the first transient kinetic investigation (to the best of our knowledge) for the MCAD-catalyzed reaction utilizing one of the most efficient (and physiological) substrates, octanoyl-CoA. The other two substrates that have been investigated in this regard are indolepropionyl-CoA (Johnson & Srivastava, 1993; Johnson et al., 1992, 1993, 1994) and butyryl-CoA (Schopfer et al., 1988; Johnson et al., 1993). Previously, we discerned that both of these substrates undergo the reductive and oxidative half-reactions via an identical sequence of steps (Johnson et al., 1993). On casual comparison of the reductive half-reaction of the enzyme utilizing octanoyl-CoA vis-à-vis IPCoA and butyryl-CoA substrates, the following differences become readily obvious. (1) Unlike IPCoA or butyryl-CoA, the octanoyl-CoA-dependent reductive half-reaction of the enzyme involves a biphasic (two-exponential) increase in absorption within the charge transfer region. With the former two substrates, the complementary reaction profiles are marked by a single-exponential increase followed by a decrease in absorbance within the charge transfer region (Johnson & Srivastava, 1993; Johnson et al., 1993; Schopfer et al., 1988). (2) The fast relaxation rate constant for the reduction of MCAD–FAD by octanoyl-CoA ($\sim$320 s^{-1}; Figure 1) is about an order of magnitude faster than the octanoyl-CoA-dependent turnover rate (11.5 s^{-1}; Beinert, 1963a) of the enzyme. This is in contrast to a comparable magnitude of these parameters involving both butyryl-CoA and IPCoA as substrates (Johnson & Srivastava, 1993; Johnson et al., 1993, 1994). In this regard, the potential of octanoyl-CoA to reduce MCAD-bound FAD at a significantly faster rate is not utilized toward enhancing the catalytic turnover of the enzyme. (3) Whereas the butyryl-CoA- and IPCoA-reduced enzyme species, e.g., MCAD–$FADH_2$–crotonyl-CoA/IACoA, are fairly susceptible to oxidation by molecular oxygen (Johnson et al., 1992, 1994), the octanoyl-CoA-reduced species, MCAD–$FADH_2$–octenoyl-CoA, is remarkably stable against oxidation by molecular oxygen; the half-life for the oxidation reaction involving the octanoyl-CoA-reduced enzyme is about 30 min. This half-life has been found to be similar to the dissociation off rate constant for the direct release of octenoyl-CoA from the MCAD–$FADH_2$–octenoyl CoA complex (our unpublished results). Hence, it appears plausible that the direct (albeit slow) dissociation of octenoyl-CoA from the MCAD–$FADH_2$–octenoyl-CoA complex produces MCAD–$FADH_2$, which is readily oxidized by O_2 (Johnson et al., 1994). The latter process is responsible for the slow oxidase activity of the enzyme when octanoyl-CoA is utilized as a substrate. In light of these observations, it is apparent that the octanoyl-CoA/octenoyl-CoA pair exhibits certain unique features during enzyme catalysis.

As is evident from the data of Figure 1, the reaction of MCAD–FAD with octanoyl-CoA results in a biphasic decrease in absorption at 450 nm and a biphasic increase in absorption at 545 nm, with similar magnitudes of the fast and slow relaxation rate constants. Since both fast and slow relaxation rate constants show a zero-order dependence on the octanoyl-CoA concentration (due to the saturation effect of octanoyl-CoA), it follows that the observed signals at 450 and 545 nm are *not* intrinsic to the formation of the E–FAD–octanoyl-CoA collision (Michaelian) complex. Thus, coupled with the precedents of the spectral features of the MCAD–FAD and MCAD–$FADH_2$–octenoyl-CoA species (Auer & Frerman, 1980), it is conceivable that the observed relaxation phases at 450 and 545 nm are due to the reduction of the enzyme-bound FAD and (with concomitant) the formation of the E–$FADH_2$–octenoyl-CoA charge transfer complex, respectively. In addition to these, the observation that the amplitudes of the absorption changes during both fast (60% of total) and slow (40% of total) relaxation phases are comparable allows us to propose a minimal model for the octanoyl-CoA-dependent reductive half-reaction of the enzyme (eq 3).

$$\text{E–FAD} + \text{OcaCoA} \underset{}{\overset{\text{very fast}}{\rightleftharpoons}} \text{E–FAD–OcaCoA} \overset{\text{fast}}{\rightleftharpoons} \text{E–FADH}_2\text{–OceCoA} \underset{}{\overset{\text{slow}}{\rightleftharpoons}} (\text{E–FADH}_2\text{–OceCoA})' \quad (3)$$

According to this model, following the formation of the E–FAD–octanoyl-CoA collision complex (via a very fast diffusion-limited process), the redox reaction generates E–$FADH_2$–octenoyl-CoA as an intermediary species, which is subsequently isomerized (presumably via a protein conformational change) to a relatively stable (E–$FADH_2$–octenoyl-CoA)′ form. Due to similarity in the magnitudes of the fast and slow relaxation rate constants, whether the reaction is measured by the disappearance of the enzyme-bound FAD (at 450 nm) or by the appearance of the reduced enzyme product (at 545 nm), it becomes evident that the conversion of E–FAD–octanoyl-CoA to E–$FADH_2$–octenoyl-CoA occurs during the fast relaxation phase, whereas the isomerization reaction of the latter (E–$FADH_2$–octenoyl-CoA) occurs during the slow relaxation phase. The kinetic profile of Figure 1 also suggests that both the redox species exhibit the property of the charge transfer complex band, albeit the extinction coefficient of the isomerized complex (X′, eq 4) is likely to be higher than that of the intermediary species (X, eq 4).

While utilizing IPCoA as a chromophoric substrate, we noticed that, within the charge transfer complex, the electronic structure of the chromophoric product, IACoA, is characterized by about a 33-nm red shift in its spectral band (final absorption maximum = 400 nm; Johnson & Srivastava, 1993). Since a qualitatively similar type of red shift is discerned upon the interaction of MCAD–FAD with IACoA, we determined that within the MCAD–$FADH_2$–IACoA charge transfer complex the carbonyl group of IACoA is polarized,

and we assigned this species to be X (Johnson & Srivastava, 1993). A kinetically identical species was detected during the reductive half-reaction of butyryl-CoA, although this species could exhibit only the charge transfer band and lacked the spectral signal characteristic of the polarized enoyl-CoA (crotonyl-CoA) moiety (Johnson & Srivastava, 1993; Schopfer et al., 1988). With these precedents, it is tempting to speculate that the first redox product of eq 3, i.e., E–$FADH_2$–octenoyl-CoA, is equivalent to X.

The question arises concerning whether the (E–$FADH_2$–octenoyl-CoA)′ complex of eq 3 is identical to the collision/Michaelian complex that is expected to be formed upon interaction of E–$FADH_2$ with octenoyl-CoA or is an isomerized form of the Michaelian complex. While contemplating this possibility, we realized that the release of octenoyl-CoA from the stable (E–$FADH_2$–octenoyl-CoA)′ complex is about 10^{-4} s^{-1} (our unpublished results), which is unusually low for the dissociation off rate constants of the enzyme-substrate/substrate analogue complexes (Hammes, 1982). This led us to suspect that the stable redox complex might be an isomerized form of the E–$FADH_2$–octenoyl-CoA collision (Michaelian) complex. This possibility was supported by the transient kinetic studies of the oxidation of E–$FADH_2$ (generated by the reduction of E–FAD in the presence of sodium dithionite) by octenoyl-CoA (data not shown). During this study, we observed that the fast relaxation rate constant for the formation of the charge transfer complex band (upon mixing E–$FADH_2$ with octenoyl-CoA) was independent of the octenoyl-CoA concentration. This suggested to us that the absorption signal during the observed relaxation phase (for the reaction in the reverse direction) might be intrinsic to the species that is generated (presumably via an isomerization step) following the formation of the E–$FADH_2$–octenoyl-CoA collision (Michaelian) complex. This was not surprising, since we had previously observed similar behavior for the interaction of E–$FADH_2$ with IACoA (Johnson & Srivastava, 1993); the Michaelian complex formed between E–$FADH_2$ and IACoA was isomerized to X, the same intermediary species that was formed during the reaction in the forward direction (Johnson & Srivastava, 1993). These facts prompt us to revise the model in eq 3 to the following form: In this model, X and X′

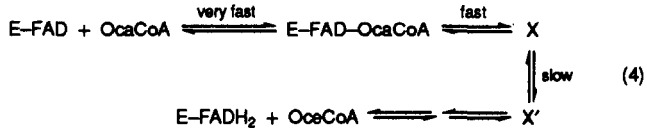

(4)

are representatives of the E–$FADH_2$–OceCoA and (E–$FADH_2$–OceCoA)′ complexes (of eq 3), respectively. It should be pointed out that although both of these species contain $FADH_2$, they differ with respect to the protein conformational states.

Due to our inability to ascertain the octanoyl-CoA concentration-dependent fast and slow relaxation rate constants for the reaction in the forward direction (see Results), we have not been able to determine the individual rate and equilibrium constants of the reaction scheme of eq 4. Nevertheless, the experimental data attest to the two following facts: (1) The binding affinities of octanoyl-CoA as well as of octenoyl-CoA for E–FAD within their respective collision complexes are fairly high. The upper limits of their dissociation constants can be set at 0.8 and 4 μM, respectively. (2) The yield of the reduced flavin species in the presence of a saturating concentration of octanoyl-CoA is dictated by the two subsequent steps, i.e., chemistry (i.e., E–FAD–octanoyl-CoA ⇌ E–$FADH_2$–octenoyl-CoA (i.e., X)), and the isomerization reaction step (i.e., X ⇌ X′). Of these, the second step appears to be unique for the substrate octanoyl-CoA, since this step was entirely absent with butyryl-CoA or IPCoA as the enzyme substrate (Johnson & Srivastava, 1993; Schopfer et al., 1988). At this point, we must mention that the maximum reductions of the enzyme-bound FAD in the presence of saturating concentrations of octanoyl-CoA, butyryl-CoA, and IPCoA are 85, 56, and 75%, respectively, due to equilibrium distribution between the oxidized and reduced forms of the enzyme species. Hence, it is tempting to speculate that the 10–30% higher yield of the reduced flavin species observed in the presence of octanoyl-CoA primarily is due to the contribution of the X to X′ isomerization step. Since the latter step is absent from reactions involving butyryl-CoA and IPCoA as substrates, the overall yields of the reduced enzyme species with these substrates are lower than those observed with octanoyl-CoA.

The spectral signals observed upon the binding of E–FAD with octenoyl-CoA (Figure 2) facilitated the transient kinetic studies for their interactions. Like the reductive half-reaction of the enzyme with octanoyl-CoA, the enzyme–octenoyl-CoA interaction was found to be biphasic at several different wavelengths (299, 394, and 440 nm), with average fast and slow relaxation rate constants of 382.3 ± 39.8 and 14.3 ± 7.4 s^{-1}, respectively. To our surprise, these values were found to be similar to the corresponding fast (319.7 ± 33.5 s^{-1}) and slow (28.8 ± 12.5 s^{-1}) relaxation rate constants observed during the reductive half-reaction of the enzyme utilizing octanoyl-CoA as the substrate. Besides, these relaxation rate constants were found to be independent of the octenoyl-CoA (between 40 and 150 μM) concentration, once again attesting to the fact that a collision complex between MCAD–FAD and octenoyl-CoA (K_d < 4 μM) was formed before the onset of the observed relaxation phases. On the basis of the fact that the observed fast and slow relaxation rate constants are similar, irrespective of whether the absorption signal was contributed by E–FAD (i.e., 450 nm) or by the E–FAD–octenoyl-CoA complex, we propose that the fast and slow relaxation steps are representative of the first and second steps (following the formation of the collision complex), respectively (eq 5).

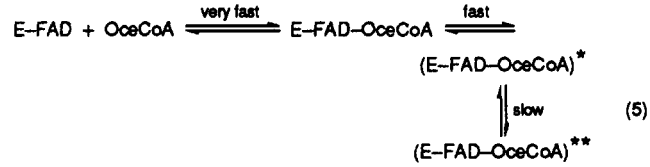

(5)

Note the marked similarity between the sequence of steps in eq 5 and that discerned during the octanoyl-CoA-dependent reductive half-reaction of the enzyme (eq 4). In both of these cases, following the formation of the enzyme–ligand collision complex (where the ligand is either octanoyl-CoA or octenoyl-CoA), two consecutive isomerization steps occur. The relaxation rate constants observed during octanoyl-CoA oxidation are similar to the corresponding rate constants observed during the octenoyl-CoA binding with MCAD–FAD. The only difference between these two seemingly diverse phenomena is that the fast (relaxation) step of eq 4 is coupled to the chemical transformation (oxidoreduction) reaction, whereas that of eq 5 is devoid of chemistry. An identical correlation was found with IPCoA/IACoA and butyryl-CoA/crotonyl-CoA as the substrate/product pairs for this enzyme, although with these pairs only one isomerization step was discerned (Johnson et al., 1994).

Further support for the similarity in the microscopic pathways of the reductive half-reaction and the enzyme–enoyl-CoA interaction comes from the off rate measurement experiments (see Figure 4). We recently have observed that octenoyl-CoA can dissociate from the MCAD–$FADH_2$–octenoyl-CoA complex via either of the two pathways. The first pathway simply involves the breakdown of the complex into MCAD–$FADH_2$ and octenoyl-CoA (the direct dissociation pathway), whereas the second pathway involves the reversal of the overall redox reaction, generating MCAD–FAD–octanoyl-CoA, followed by breakdown of the latter complex into MCAD–FAD and octanoyl-CoA (the indirect dissociation pathway; eq 6A). Due to a favorable energetic barrier, the latter pathway is more facile than the former (our unpublished results). However, in the case of the MCAD–FAD–octenoyl-CoA complex, the only pathway for the dissociation of octenoyl-CoA is the reversed sequence of eq 5 (analogous to the indirect dissociation pathway mentioned above; eq 6B). Hence, upon mixing E–$FADH_2$–octenoyl-CoA or E–FAD–octenoyl-CoA with excessive concentrations of acetoacetyl-CoA, the following sequence of steps can be envisaged:

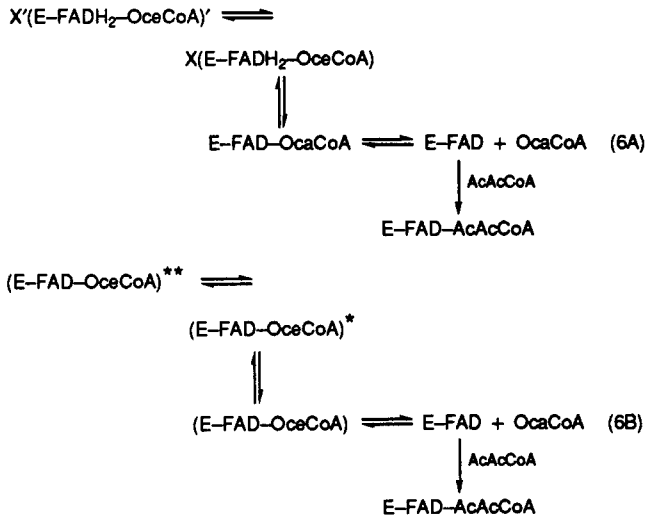

The observed rate constants for the formation of the E–FAD–acetoacetyl-CoA complex were found to be 7.1 ± 0.1 and 10.3 ± 0.2 s^{-1} for the displacement reactions of eqs 6A and 6B, respectively. These rate constants are remarkably similar, particularly considering the fact that the two processes of eq 6 are quite diverse. These observations are suggestive of the fact that although the two processes are conceptually different (i.e., chemical transformation versus physical interaction), they proceed via a common microscopic pathway. We are currently testing the generality of this hypothesis with different acyl-CoA/enoyl-CoA pairs, and we will report these findings subsequently.

The above-noted similarities initially led us suspect that our octenoyl-CoA preparation might be contaminated by octanoyl-CoA and that this contamination was responsible for a near-equality in the relaxation rate constants during the two diverse processes. However, this possibility was readily ruled out by the fact that the kinetic pattern for the MCAD–FAD + octenoyl-CoA interaction was the same at different wavelengths (see Figure 1A). This was particularly so at 394 nm, where the signal for the interaction between MCAD–FAD and octenoyl-CoA was marked by an increase (rather than a decrease, in the case of octanoyl-CoA) in the absorption of the flavin band (see Figure 2). In addition, we performed experiments in which the octenoyl-CoA preparation was deliberately contaminated with 5% octanoyl-CoA. In the latter case, an increase followed by a (slow) decrease in absorption at 394 nm was observed, which was not observed with the octenoyl-CoA preparation that was free from octanoyl-CoA contamination (data not shown). These results, coupled with our repeated observations that the octenoyl-CoA preparation eluted as a symmetrical peak (with no shoulder near the octanoyl-CoA elution region) from a C_{18} HPLC analytical column, compel us to believe that the relaxation rate constants obtained for the interaction of MCAD–FAD with octenoyl-CoA are indeed similar to those observed for the reaction of MCAD–FAD with octanoyl-CoA.

The question arises concerning why the two functionally diverse processes, i.e., the enzyme-catalyzed chemical transformation versus the enzyme–ligand interaction, conform to an identical sequence of steps with similar equilibration rate profiles. If the latter is a reflection of the near-equality in the individual (forward and reverse) rate constants of the corresponding relaxation steps, it would mean that the energetics of both these processes are the same. This may further imply that the corresponding ground and transition states of these two processes have identical free energies. Does it mean that the putative transition state structures formed during the reductive half-reaction of octanoyl-CoA and those formed during the electronic structural changes of the oxidized flavin upon interaction with octenoyl-CoA are the same? Although it may appear unlikely, our experimental data demand such a possibility according to transition state theory (Connors, 1990).

Having been puzzled by many analogous instances, Bernhard (1981) advocated stringent roles for the protein conformational changes during enzyme–ligand interactions and enzyme catalysis. In light of Bernhard's theory, the MCAD protein must exist in ligand-dependent alternative conformation states (e.g., E_1, E_2, E_3, etc. of eq 7), and the transition between these conformational states must be intimately coupled to the changes in the bond structures of the ligands. Hence, the driving force of either the chemical transformation (e.g., eq 4) reaction or the electronic structural changes (e.g., eq 5) is the protein conformational changes, as illustrated by eq 7. The possibility of the existence of alternative conformational states of the enzyme must await X-ray crystallographic investigations of the enzyme–ligand complexes to atomic resolution (Kim et al., 1993). We are currently assessing the validity of this hypothesis for this and other enzymes under investigation in our laboratory.

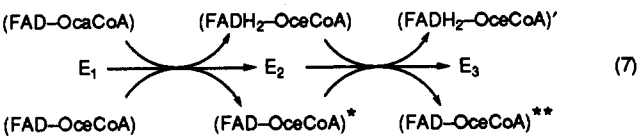

REFERENCES

Auer, H. E., & Frerman, F. E. (1980) *J. Biol. Chem. 255*, 8157–8163.
Beinert, H. (1963a) *The Enzymes (2nd Ed.) 7*, 447–466.
Beinert, H. (1963b) *The Enzymes (2nd Ed.) 7*, 467–476.
Beinert, H., & Page, E. (1957) *J. Biol. Chem. 225*, 479–497.
Bernert, J. T., & Sprecher, H. (1977) *J. Biol. Chem. 252*, 6737–6744.
Bernhard, S. A. (1981) *Stud. Org. Chem. (Amsterdam) 10*, 237–252.
Connors, K. A. (1990) *Chemical Kinetics: The Study of Reaction Rates in Solution*, VCH Publishers, Inc., New York.

Crane, F. L., Mii, S., Hauge, J. G., Gree, D. E., & Beinert, H. (1956) *J. Biol. Chem. 218*, 701–716.
Ellman, G. L. (1959) *Arch. Biochem. Biophys. 82*, 70–77.
Engel, P. C. (1990) in *Chemistry and Biochemistry of Flavoenzymes* (Muller, F., Ed.) Vol. III, pp 597–655, CRC Press, Inc., London.
Hall, C. L., Lambeth, J. D., & Kamin, H. (1979) *J. Biol. Chem. 254*, 2023–2031.
Hammes, G. G. (1982) *Enzyme Catalysis and Regulation*, Academic Press, New York.
Johnson, J. K., & Srivastava, D. K. (1993) *Biochemistry 32*, 8004–8013.
Johnson, J. K., Wang, Z., & Srivastava, D. K. (1992) *Biochemistry 31*, 10564–10575.
Johnson, J. K., Kumar, N. R., & Srivastava, D. K. (1993) *Biochemistry 32*, 11575–11585.
Johnson, J. K., Kumar, N. R., & Srivastava, D. K. (1994) *Biochemistry 33*, 4738–4744.
Kim, J. P., Wang, M., & Paschke, R. (1993) *Proc. Natl. Acad. Sci. U.S.A. 90*, 7523–7527.
McFarland, J. T., Lee, M., Reinsch, J., & Raven, W. (1982) *Biochemistry 21*, 1224–1229.
McKean, M. C., Frerman, F. E., & Mielke, D. M. (1979) *J. Biol. Chem. 254*, 2730–2735.
Murfin, W. W. (1974) Ph.D. Dissertation, Washington University, St. Louis, MO.
Schopfer, L. M., Massey, V., Ghisla, S., & Thorpe, C. (1988) *Biochemistry 27*, 6599–6611.
Thorpe, C., Matthews, R. G., & Williams, C. H., Jr. (1979) *Biochemistry 18*, 331–337.
Yao, K.-W., & Schulz, H. (1993) *Anal. Biochem. 214*, 528–534.